The cold and the drought: effects of extreme weather events on Stem Carbon dynamic in a Mediterranean beech forest

Ettore D'Andrea[1*], Negar Rezaie[1*], Peter Prislan[2], Jan Muhr[3,4], Alessio Collalti[5,6], Giorgio Matteucci[1], Jozica Gričar [2]

[1]CNR-ISAFOM, via Patacca 2, 80056 Ercolano (NA), Italy

[2]Department of Yield and Silviculture, Slovenian Forestry Institute,SI-1000 Ljubljana, Slovenia

[3]University of Göttingen, Bioclimatology, Büsgenweg 2, 37077 Göttingen, Germany

[4]Max-Planck-Institute for Biogeochemistry, Department of Biogeochemical Processes, Hans-Knoell-Str. 10. 07745 Jena, Germany

[5]CNR-ISAFOM, Via Cavour 4/6, 87036, Rende (CS), Italy

[6] Department of Innovation in Biological, Agro-food and Forest Systems, University of Tuscia, 01100 Viterbo, Italy

*Corresponding Authors:

ettore.dandrea@isafom.cnr.it, +393389119720

rezaie.negar@gmail.com, +393349410230

Total words: 5360

Introduction: words:906

Materials and Methods: word:1693

Results: words:1342

Discussion: words:1419

Acknowledgements: words:79

Figures:6, **colour figures**:5

Tables:3

Summary

The effects of short-term extreme events on tree functioning are still rather elusive. Considering beech one of the most sensible species to late frost and water shortage, we investigate the intra-annual C dynamics in stems under such conditions. Wood formation and stem CO_2 efflux were monitored in a Mediterranean beech forest for three years (2015−2017) which were characterized by a late frost (2016) and a summer drought (2017). The late frost event reduced radial growth and consequently the amount of carbon fixed in the stem biomass by 80%. Stem carbon efflux in 2016 was reduced by 25%, which can be attributed to reduced effluxes due to growth respiration. Consequently, the amount of carbon emitted was higher than the carbon fixed in stems, causing an net emission of 0.468 Mg C ha^{-1} yr^{-1}. Counter to our expectations, we found no effects of the 2017 summer drought on radial growth and stem carbon efflux.

Even if forests are potentially susceptible to all weather extremes, which are becoming more frequent in Mediterranean basin, the study evidenced the negative effect of spring late frost but the high resilience of beech that resumed the growth in 2017, and became again C sink.

Keywords: *Fagus sylvatica* L. (beech), late frost, extreme weather event, wood formation, stem carbon efflux, resilience, drought, growth.

Introduction

Even small changes in the mean or variance of a climate variable cause disproportionally large changes in the frequency of extreme weather events, recognized as major drivers of current and future ecosystem dynamics (Frank *et al.*, 2015). In the near future, Mediterranean region is predicted to be the most vulnerable to global change between the European regions (Schröter *et al.*, 2005). Changes in temperature and precipitation regimes may increase drought risk (Schröter *et al.*, 2005), which can negatively affect physiological performance (Rezaie *et al.*, 2018), growth and competitive strength (Peuke *et al.*, 2002) of common beech, one of the most important and widespread broadleaved trees in Europe.

Increasing spring temperatures can trigger earlier leaf unfolding (Gordo & Sanz, 2010; Allevato *et al.*, 2019), which in turn results in higher risk that young leaves are exposed to spring frost, especially at higher elevation (Vitasse *et al.*, 2018). Temperatures below −4°C can kill the developing new shoots and leaves, thus reducing the photosynthetic area and ultimately the trees' growth. In addition, depending on the intensity of damage, the formation of new leaves requires a high amount of reserves (Dittmar *et al.*, 2006; D'Andrea *et al.*, 2019).

Tree stems play an important role in the carbon balance of forest ecosystems (Yang *et al.*, 2016). Part of the carbon (C) fixed by photosynthesis is allocated to stem, while some is respired by stems and emitted into the atmosphere. Radial growth – an often used proxy for the overall allocation of C to the stem (Bascietto *et al.*, 2004; Cuny *et al.*, 2015; Chan *et al.*, 2018a) – is largely related to the process of wood formation, which can be divided into five (main) developmental phases: *i*) cambial cell division; *ii*) cell enlargement; *iii*) secondary wall deposition and *iv*) cell wall thickening (lignifications); while *v*) in the case of vessels and fibres, also genetically-programmed cell death or apoptosis (Prislan *et al.*, 2018). The whole process is sensitive to many factors as leaf phenology (Michelot *et al.*, 2012), temperature (Begum *et al.*, 2007), drought (Linares *et al.*, 2009), tree-size and social status (Rathgeber *et al.*, 2011), and tree vigour (Gričar *et al.*, 2009).

As also described by Damesin (2003), the only current-year stem respiration may represent the 8% of the overall above ground respiration and 1.4% of the annual carbon assimilation. A recent global estimate shows that the only stem respiration from boreal to tropical forests combined was 6.7 (± 1.1) Pg C yr^{-1}, which corresponds to 84% of the mean annual anthropogenic emission (Yang *et al.*, 2016). Measurements of actual stem respiration (RS) are difficult if not impossible (Teskey *et al.*, 2008), and the most commonly measured proxy, namely stem CO_2 efflux (ES), is likely to underestimate local respiration (Trumbore *et al.*, 2013). Still, previous studies reported a strong correlation between RS and ES, with ES ranging between 82–94% and 86–91% of RS in *Populus deltoides* (Saveyn *et al.*, 2008) and *Dacrydium cupressinum* Lamb stems (Bowman *et al.*, 2005), respectively. Another study using O_2 uptake as an alternative proxy for actual respiration and comparing it to traditionally measured ES, showed that ES on average underestimated RS by about 41% (CO_2 was not emitted locally at the point of measurement) (Hilman *et al.*, 2019). ES and RS are different because part of the CO_2 produced by respiration is not released directly through the bark in atmosphere, but it is dissolved in xylem sap and is carried upward by the transpiration stream (Bloemen *et al.*, 2014). In addition, ES is affected by CO_2 deriving from root respiration which is carried upward into the stem (Bloemen *et al.*, 2013). Moreover, part of respired CO2 can be fixed in the xylem storage pools (Ubierna *et al.*, 2009)

ES proved to be related to stem temperature, growth rates, distribution and turnover of living cells (Collalti *et al.*, 2019) nitrogen concentration (Ceschia *et al.*, 2002), to tree social class (Guidolotti *et al.*, 2013) and varies seasonally due to growth (Gruber *et al.*, 2009). ES is affected by growth respiration, which provides the energy for synthesizing new tissues; and by maintenance respiration, which maintains existing living cells (Ceschia *et al.*, 2002).

Separating ES into these components allows for further investigation of stem carbon budgeting and tissue costs (Chan *et al.*, 2018b). Not much is known on the interaction between wood formation (xylogenesis) and ES and a deeper investigation of this link is crucial, especially in the context of climate change and extreme weather events, which may greatly modify the contribution of these processes to C cycle. Nevertheless, despite the crucial role of extreme events and the rising attention to their prospected increasing role in future climate scenarios, information on the effect of short-term extreme events on tree functioning is still rather elusive (Carrer *et al.*, 2016; Gazol *et al.*, 2019).

In this context, we monitored xylogenesis together with ES in a Mediterranean beech forest from 2015 to 2017 – a period characterized by a spring late frost (2016) and a summer drought (2017) – with the objective to unravel the intra-annual C dynamics in stems under these two extreme weather events. We hypothesized that: 1) cambial activity and radial growth may cess soon after leaf death due to 2016 spring late frost; 2) second leaf re-sprouting may start at the expense of stem growth; 3) 2017 summer drought negatively impact stem biomass production and effluxes; and that 4) such extreme weather events would alter the stems C dynamic at both tree and stand scale.

Material and methods

Study site

The measurements were carried out between 2015 and 2017 on a long-term monitored beech stand *(Fagus sylvatica* L.) located at Selva Piana (41°50'58" N, 13°35'17" E, 1,560 m elevation) close to Collelongo (Abruzzi Region, Italy) in the Central Apennine. Site information regarding forest structure, climate and soil are all in depth described in previous works (Chiti *et al.*, 2010; Guidolotti *et al.*, 2013; Collalti *et al.*, 2016; Rezaie *et al.*, 2018).

In the night between 25th and 26th of April 2016 (Day Of Year, DOY 115), a spring late frost occurred in Central and South Italy, causing leaf damage in many beech stands (Bascietto *et al.*, 2018; Greco *et al.*, 2018; Nolè *et al.*, 2018; Allevato *et al.*, 2019). In the Selva Piana site the air temperature reached – 6°C at canopy level, destroying the whole-stand canopy and leaving the trees without leaves for almost two months. The 2017 growing season was characterized by a prolonged summer drought, starting in June and getting more severe over the next two months. In 2017, annual precipitation was 950 mm, with only 54 mm of precipitation from June to August. The daily maximum average temperature was 23.9 °C in

August 2017, ~ 2°C warmer than the long-term average (1950–2013) (**Error! Reference source not found.**).

Tree selection, wood formation dynamic and xylem phenology

Sampling was performed on five trees (Rezaie *et al*., 2018), that were selected for their similarity with site tree ring chronology, as done in other studies on wood formation and stem CO_2 efflux (Ceschia *et al*., 2002; Damesin *et al*., 2002; Gruber *et al*., 2009; Delpierre *et al*., 2019). Micro-cores collection, and cross-sections preparation followed the standard methodology described in Prislan *et al.* (2013). On each photographed cross-section, the number of cambium cells was counted, and the widths of the developing xylem were measured along three radial directions. The dynamics of xylem formation were analyzed by fitting Gompertz function to xylem increments (Prislan *et al*., 2018; Rathgeber *et al*., 2018), corrected for the previous tree ring width (Oladi *et al*., 2011), as follows:

$$y = \alpha \exp\left[-e^{(\beta - kt)}\right] \quad (1)$$

where y is the cumulative ring width (μm) at time t (day of the year), α is the final asymptotic size representing the annual potential growth, β is the x-axis placement parameter, and k is the rate of change parameter.

For each tree and monitoring year the following phenological xylem formation phases were recorded: *i*) cambium *reactivation*, *ii*) beginning of cell *enlargement* period (bE); *iii*) beginning of cell wall *thickening* (bW); *iv*) beginning of cell *maturation* (bM); *v*) *cessation* of cell enlargement phase (cE); and *vi*) cessation of cell wall thickening and *lignification* phase (cW). The date of cambium reactivation was assessed as the average between dates when an increase of cambium cells was observed (i.e. from 3-4 to 6-7 cells in a radial row) (Čufar *et al*., 2008; Deslauriers *et al*., 2008). Phases of xylem growth and ring formation were computed using logistic regressions, spanning from the 50% probability that phenophase have started or ended (Rathgeber *et al*., 2018). Based on phenological phases, the duration of key wood formation phases were calculated: *i*) the overall duration of the enlargement period (*d*E = cE – bE); *ii*) the duration of the wall-thickening period (*d*W = cW – bW); and *iii*) the total duration of wood formation (i.e. the duration of xylogenesis) (*d*X = cW – bE). Data were analysed using the CAVIAR (v2.10-0) package (Rathgeber *et al*., 2018) built for R statistical software (R Development Core Team, 2018).

Starting from the detailed time-resolved data from tree micro-cores, the annual C fixed in the stem (SG_t) was estimated for each sampled tree as follows:

$$SG_t = \frac{0.46 \times (BS_t - BS_{t-1})}{\Delta t} \quad (2)$$

Where SG_t is the amount of C fixed in stem per year expressed in Mg C yr^{-1}, 0.46 is the carbon content of the woody tissues (Scarascia-Mugnozza *et al.*, 2000), BS_t and BS_{t-1} are the stem biomass in Mg of Dry Matter (DW) of at the beginning and at the end of each sampling year, Δt is the time variation (one year).

The site-specific allometric equation for beech used for BS was that proposed by Masci (2002):

$$BS = \frac{283.734 \times DBH^{2.134}}{10^6} \quad (3)$$

Where BS is in Mg DW, and DBH is the diameter (in cm) at 1.30 m (R^2 = 0.96, *p*-value < 0.01).

Stem CO_2 efflux (ES)

Two PVC collars (10 cm diameter and 5 cm high, one facing north and one south) were fixed on each tree with flexible plastic ties and sealed leak tight with Terostat (Henkel KgaA, Germany). When present, bark mosses and lichens were removed. Stem CO_2 efflux was measured with a portable IRGA (EGM 4, PP-System, Hitchin, UK), equipped with a closed-dynamic chamber (SRC-1, PP-System, Hitchin, UK), that was tighted to the collars. Each measurement consisted of a 120 seconds loop, where CO_2 concentration inside the chamber was measured every 5 seconds. During measurements the CO_2 concentration typically increased by 10 to 50 µmol mol^{-1}.

Stem CO_2 efflux (ES) was calculated as:

$$ES = K_{CO_2} \div V_{mol} \times \frac{V_{cuv}}{A} \quad (4)$$

ES is stem CO_2 efflux per surface area (µmol m^{-2} s^{-1}), K_{CO2} (µmol $mol^{-}1$ s^{-1}) is the slope of the regression between CO_2 concentration and time during measurements, V_{mol}, the molar volume, is the volume occupied by one mole of CO_2 (m^3 mol^{-1}), at the air pressure (measured

by built-in sensor of the EGM-4) and air temperature (T_{air}, °C) at measurement time, *A* is the exposed lateral area of stem (m^2), and V_{cuv} is the sum of SRC-1 and collar volumes (m^3). Temperature was used to calculate the relationship among ES and T_{air}, using the well-known Arrhenius exponential function:

$$ES = a \times e^{Tair \times b} \quad (5)$$

ES overall temperature sensitivity for a 10 °C increase (Q_{10}) was calculated according to Gruber *et al*. (2009) as:

$$Q_{10} = 10^{K_T \times 10} \quad (6)$$

where K_T is the regression slope taken from linear regression of log10 of ES versus T_{air}.

From the wood formation and xylem phenology analysis described above, we identified wood (*w*) and non wood (*nw*) formation periods for each tree, so it was possible to separate the measured ES in two groups, ES_w and ES_{nw}. Thus, according to Eq. 5, we calculated per each group the specific CO_2 efflux at a base air temperature of 15°C (ES_{15w} and ES_{15nw}) and the specific Q_{10} (Q_{10w} and Q_{10nw}).

During the non-wood formation period, ES_{nw} is constituted only by the effluxes derived by the maintenance respiration (ESb, µmol m^{-2} s^{-1}) that was calculated as:

$$ES_{nw} \equiv ESb = ES_{15nw} \times Q_{10nw}^{\frac{(T_{air}-15)}{10}} \quad (7)$$

During the wood formation period ES_w (µmol m^{-2} s^{-1}), which is affected by both maintenance and growth respiration, was calculated as:

$$ES_w = ES_{15w} \times Q_{10w}^{\frac{(T_{air}-15)}{10}} \quad (8)$$

We assumed that ESb and its relationship with air temperature was also valid during wood formation period, although this approach is not accounting for the acclimation of maintenance respiration to temperature during warmer periods. Nevertheless, there are contrasting hypotheses on this process (Carey *et al*., 1997; Stockfors & Linder, 1998). Under this

assumption, we calculated the stem CO_2 efflux due to growth respiration, ESg (μmol m^{-2} s^{-1}), as:

$$ESg = ES_w - ESb \quad (9)$$

The daily C effluxes of the whole stem were obtained by integrating, over the entire stem area, the effluxes through equation 7, 8, 9, using the half-hourly T_{air} values measured at the site. The stem area was calculated as follow:

$$LA = 0.464 \times DBH - 2.083 \quad (10)$$

where LA is the stem lateral area (m^2) and DBH is the stem diameter (in cm) at 1.30 m (R^2 = 0.828, *p*-value < 0.01, for more details on equation see additional material). Using this approach, we considered the measurement at 1.30 m representative of the whole stem, even if contrasting effect of height on stem CO_2 effluxes are reported (Damesin *et al*., 2002; Katayama *et al*., 2019).

Annual values of each C fluxes of the five sampled trees (TES, TESb, TESg, see Table 1 for definitions) were obtained summing up the daily values.

From tree to stand level

Annual values of each fluxes per tree at stand scale (ASG, AESb, AESw, AESg) were estimated using a probabilistic sampling scheme that yields unbiased estimators for several variables (Bascietto *et al.*, 2004, 2012) .

DBH elevated to the power of 2.5 ($DBH^{2.5}$) (Bascietto *et al.*, 2012) was used as proxy variable to estimate stem C fluxes. The sampling probability at the stand level (P_{t_j}) of the j_{th} tree was calculated as

$$P_{t_j} = \frac{A_{t_j}}{\sum_{j=1}^{q} A_{t_j}} \quad (11)$$

where q is the number of trees in the stand, and A_{tj} is the proxy variable ($DBH^{2.5}$) of the j_{th} tree. Every j_{th} tree yields an unbiased estimator of stem fluxes of the stand:

$$\widehat{V_{S_j}} = \frac{W_{C_j}}{P_{t_j}} \quad (12)$$

Where W_{C_j} is the stem flux (e.g. TES, TESb, TESg, and SG) of the j_{th} tree. Consequently, it is possible to calculate the unbiased mean and the variance of the estimator, as follow:

$$\widehat{V_S} = \frac{1}{n} \times \sum_{j=1}^{n} \widehat{V_{S_j}} \quad (13)$$

$$\sigma^2\left(\widehat{V_S}\right) = \frac{\sum_{j=1}^{n}\left(\widehat{V_{S_j}} - \widehat{V_S}\right)^2}{n \times (n-1)} \quad (14)$$

Where *n* is the number of sampled trees.

Meteorological and phenological data

Half-hourly air temperature and precipitation were downloaded by ERA5 database of the European Centre for Medium-Range Weather Forecasts (ECMWF) (https://www.ecmwf.int/en/forecasts/datasets/archive-datasets/reanalysis-datasets/era5), and downscaled to experimental site using relationships built using previously measured values for temperature (°C) and precipitation (mm). Comparison against data measured at the site confirm the reliability of this choice that allows to use a continuous data series, without gaps. Leaf phenology was monitored using the MODIS Leaf Area Index product (LAI, MOD15A2H, https://modis.gsfc.nasa.gov/) with 8-day temporal resolution and 500 meter spatial resolution. The date of onset of photosynthetic activity (green up) and the date at which plant green leaf area peaks its annual maximum (maturity) were assessed trough the rate of change in the curvature of the fitted logistic models (Zhang *et al.*, 2003).

Statistical data analysis

Descriptive parameters of the growth and xylem phenology were tested using One Way Repeated Measures Analysis of Variance, considering years as factor, followed by post-hoc (Holm-Sidak method). Exponential equation was used to evaluate the relationship between ES and T_{air}. Differences among ES parameters (Q_{10} and ES_{15}) were tested using Two Way Repeated Measures ANOVA (Two Factor Repetition), using year and period (non-wood formation, wood formation) as factors. Multiple comparisons were performed by Holm-Sidak method. Linear regressions were used to assess the relationship between ESg and SG. We tested data normality and constant variance using Shapiro-Wilk test and the Spearman rank correlation between the absolute values of the residuals and the observed value of the dependent variable, respectively.

Results

Wood formation dynamic

The date of onset of photosynthetic activity, based on leaf area index (LAI) dynamics, differed among the study years, occurring at DOY 118, 95, and 127 in 2015, 2016 and 2017,

respectively. In all three years, cambium activation occurred after leaf unfolding at DOY 123 ± 4, 118 ± 8, 138 ± 6 in 2015, 2016 and 2017, respectively (Fig. 1). In 2016, cambium cell production continued also after the late frost event, but at considerably lower rates.

Different intra-annual growth patterns were observed during the three study years, especially in the year of the late frost (2016, Fig. 2, Table 1). In 2016, the maximal growth rate (rx) ($F = 8.469$, p-value = 0.014) was lower and was reached 3 weeks earlier (tx) ($F = 22.667$, p-value < 0.001) than in the other two years. The different intra-annual growth patterns resulted also in significantly narrower tree rings in 2016 (230.12 ± 1.54 µm) ($F = 13.272$, p-value < 0.01) than in 2015 (1312.17 ± 196.15 µm) and 2017 (1234.80 ± 269.32 µm).

In the study years, differences were also observed for the beginning, cessation, and duration of wood formation phases (Fig. S2). The beginning of the enlargement phase occurred earliest in 2016 and latest in 2017 ($F = 34.789$, p-value < 0.001). In contrast, the cessation of this phase was observed latest in 2015 ($F = 17.155$, p-value < 0.01). Consequently, the duration of the enlargement phase was longer in 2015 (110 ± 22 days) than in 2016 (82 ± 4 days) and 2017 (78 ± 4 days) ($F = 8.025$, p-value = 0.01). The beginning of wall thickening phase did not differ among the years ($F = 4.188$, p-value = 0.06). The cessation of this phase occurred latest in 2015 ($F = 69.167$, p-value < 0.001). Thus, the duration of wall thickening phase was shorter in 2016 (57 ± 5 days) than 2015 (99 ± 6 days) and 2017 (75 ± 4 days) ($F = 26.561$, p-value < 0.001). We observed also a delay in the beginning of the maturation phase in 2016 (at DOY 200 ± 4) with respect to 2015 (at DOY 178 ± 4) and 2017 (at DOY 176 ± 2) ($F = 11.650$, p-value < 0.01). The overall duration of wood formation was longer in 2015 (128 ± 5 days) than in 2016 (98 ± 8 days) and 2017 (97 ± 8 days) ($F = 12.561$, p-value < 0.001).

Stem CO_2 efflux (ES)

During the monitoring period (April 2015 – November 2017), the measured ES ranged between 0.16 ± 0.03 µmol CO_2 m^{-2} s^{-1} (December 2015) and 3.01 ± 0.40 µmol CO_2 m^{-2} s^{-1} (August 2017) (Fig. 3). Mean ES measured in 2016 (0.68 ± 0.19 µmol CO_2 m^{-2} s^{-1}) was lower ($F = 24.476$, p-value < 0.01) than in 2015 (1.11 ± 0.40 µmol CO_2 m^{-2} s^{-1}) and 2017 (1.29 ± 0.30 µmol CO_2 m^{-2} s^{-1}).

In each years, ES was strongly related to air temperature through the standard exponential function (Fig. 4). The relation was confirmed at the different aggregation level of measurements (whole year, wood formation and non-wood formation periods; see also Table S2 in Supporting Information).

Q_{10} shown to be 2.71 ± 0.15, 2.11 ± 0.18, and 2.68 ± 0.15, in 2015, 2016, and 2017, respectively. The Q_{10} parameter was not strongly affected by the sampling year (*p*-value = 0.059), although the values in 2016 were 22% lower than the other two years. Wood formation affected the Q_{10} parameter (F = 31.563, *p*-value < 0.01) with Q_{10w} and Q_{10nw} calculated to be 3.06 ± 0.15 and 1.93 ± 0.14 (t = 5.571, *p*-value < 0.01), respectively. This difference was confirmed for all of the sampled years.

Also ES_{15} was affected by the different conditions of monitoring years (F = 7.094, *p*-value = 0.01) with mean values of 2016 (0.63 ± 0.07 µmol CO_2 m^{-2} s^{-1}) lower than 2015 (0.93 ± 0.12 µmol CO_2 m^{-2} s^{-1}) and 2017 (0.82 ± 0.12 µmol CO_2 m^{-2} s^{-1}). Similarly to Q_{10}, wood formation period affected also ES_{15}, with ES_{15w} (0.84 ± 0.22 µmol CO_2 m^{-2} s^{-1}) higher than ES_{15nw} (0.73 ± 0.02 µmol CO_2 m^{-2} s^{-1}, F = 7.094, *p*-value = 0.01). Furthermore, during the wood formation period, ES_{15w} was higher in 2015 (1.03 ± 0.07 µmol CO_2 m^{-2} s^{-1}) and 2017 (0.90 ± 0.07 µmol CO_2 m^{-2} s^{-1}) than in 2016 (0.60 ± 0.09 µmol CO_2 m^{-2} s^{-1}). No differences among years were found for ES during the non-wood formation periods.

Annual ES for individual trees ranged between 112 g C m^{-2} yr^{-1} in 2016 (tree 4) and 349 g C m^{-2} yr^{-1} in 2017 (tree 2). Average total ES for all sampled trees was lower in 2016 (182 ± 25 g C m^{-2} yr^{-1}, F = 12.007, *p*-value < 0.01) than in 2015 (258 ± 27 g C m^{-2} yr^{-1}) and 2017 (233 ± 35 g C m^{-2} yr^{-1}).

The estimated contribution of maintenance respiration to ES for individual trees ranged between 112 g C m^{-2} yr^{-1} in 2016 (tree 4) and 284 g C m^{-2} yr^{-1} in 2017 (tree 2), and was lower, on average, in 2016 (169 ± 21 g C m^{-2} yr^{-1}) than in 2015 (211 ± 18 g C m^{-2} yr^{-1}) (q = 5.104, *p*-value = 0.017).

Likewise, the estimated contribution of wood formation to ES for individual trees varied between 0 in 2016 (tree 4) and 70 g C m^{-2} yr^{-1} in 2015 (tree 2) and was significantly lower (F = 8.144, *p*-value = 0.012) on average in 2016 (14 ± 5 g C m^{-2} y^{-1}) than in 2015 (48 ± 9 g C m^{-2} yr^{-1}) and 2017 (39 ± 8 g C m^{-2} yr^{-1}). In relative terms, contribution to ES by wood formation was estimated to be 18 ± 2%, 9 ± 3%, and 16 ± 3% in 2015, 2016, and 2017, with the remaining CO_2 efflux originating from maintenance respiration.

Radial growth and stem C effluxes

During the study period, annual average measured ES and tree ring widths were closely related (Fig. 5). Seasonal patterns of ES were similar in the three experimental years, but with different amplitudes (Fig. 6). Moreover, ESb, the stem C effluxes affected by maintenance respiration, showed a similar pattern among the three years. We observed a time-lag between

353 the time of maximum growth rate (tx) and maximum ES values of 23 ± 2 days, 31 ± 2 days,
354 and 29 ± 1 days in 2015, 2016, and 2017, respectively. Differences between years were not
355 significant (F = 3.317, *p*-value = 0.07).

356 ***From tree to stand level***

357 Annual stand-level stem C emission (AES) was lower in 2016 (0.7 ± 0.01 Mg C ha^{-1} yr^{-1})
358 than 2015 (0.9 ± 0.1 Mg C ha^{-1} yr^{-1}) and 2017 (0.9 ± 0.1 Mg C ha^{-1} yr^{-1}) (Table 3). During
359 the experimental years, annual stem C effluxes due to maintenance respiration (AESb) were
360 similar; in contrast AES due to growth respiration (AESg) was lower in 2016 (0.05 ± 0.01 Mg
361 C ha^{-1} yr^{-1}) than in 2015 (0.18 ± 0.03 Mg C ha^{-1} yr^{-1}) and 2017 (0.14 ± 0.02 Mg C ha^{-1} yr^{-1}).
362 The contribution of AESg to the annual stem effluxes was 26%, 2%, and 24% in 2015, 2016,
363 and 2017, respectively.
364 The amount of carbon fixed in stem biomass (SG) was lower in 2016 (0.2 ± 0.05 Mg C ha^{-1}
365 yr^{-1}) compared to 2015 (1.1 ± 0.1 Mg C ha^{-1} y^{-1}) and 2017 (1.0 ± 0.2 Mg C ha^{-1} yr^{-1}). The
366 difference between SG and AES was positive in 2015 and 2017, but negative in 2016. At the
367 studied beech forest, the mean C construction cost of wood, assessed as the slope of the
368 relationship between AESg and SG at tree level (R^2 = 0.849, *p*-value < 0.01, see supporting
369 information Fig.S3), was 0.2 g C emitted per g C fixed. This parameter was the mean between
370 years being 0.15 ± 0.01 for 2015, 0.25 ± 0.06 for 2016, and 0.13 ± 0.06 for 2017, respectively.

371 ## Discussion

372 ***Cambial activity and radial growth are not entirely linked to leaf phenology***

373 To the best of our knowledge, for the first time the effects of a spring late frost and a
374 subsequently close summer drought on the wood formation of beech were described.
375 In all three years, cambium reactivation and wood formation occurred within 1-3 weeks after
376 leaf development, confirming the tight dependence of the radial growth on leaf phenology and
377 photosynthesis in diffuse-porous species (Čufar *et al.*, 2008; Michelot *et al.*, 2012).
378 Nevertheless, in diffuse-porous trees, stem conductivity to water occurs in several outermost
379 growth rings and is not limited to the youngest formed xylem, as in ring-porous species
380 (Schume *et al.*, 2004). Hence, in beech allocation to current year wood is not as decisive as in
381 ring-porous species, and newly formed photosynthates at the beginning of the season are
382 rather used for other crucial processes, such as foliage and fine root growth. At the same site,
383 Matteucci (1998) analysed in parallel net ecosystem exchange (NEE) and carbon allocation to
384 foliage and wood growth (dendrometers), finding that the latter started approximately 15 days
385 after photosynthesis exceeded respiration (i.e. NEE was negative). Until then, net absorbed

carbon was allocated mostly to foliage growth. This can be related to C allocation hierarchy that identifies newly developing leaves as the main C sink as at the beginning of the growing season (Campioli *et al*., 2013; Collalti *et al*., 2018; Merganičová *et al*., 2019, and references therein). Interestingly, and counter to our expectations, in 2016 the cambium remained active at low rates even after complete canopy defoliation. D'Andrea *et al*. (2019) already showed that in the absence of photosynthesis old C reserves fuelled leaves production and likely other physiological activities of the tree. In the present work we found that also cambium activity, besides a second leaf production, behaves as an additional C sink, giving new insight on tree internal C regulation and the pivotal role of C reserve.

After the second re-sprouting, the cambium cell production decreased and became non-productive, although the environmental conditions were still favourable for radial growth. Stem radial growth of beech in Selva Piana was greatly affected by extreme late spring frost event in 2016 because of the premature cessation of cambial cell production and the lower growth rate during the active period, which resulted in 82% narrower annual xylem increments if compared to 2015 and 2017. This can be related to a somewhat hypothesised, genetically controlled, form of hierarchy in C allocation (composed by old C reserve and recently fixed photosynthetates) that identifies newly developing leaves as the main C sink rather to radial growth (Campioli *et al*., 2013; Collalti *et al*., 2018; Merganičová *et al*., 2019). Some new insights on the genetic control (rather than the environmental ones) on cambial growth have only emerged recently (see Zhang *et al*. 2019; Greb, 2019) but a clear picture still missing. In beech, previously reported growth reduction, as a consequence of late frost, ranged from 48 to 83% in beech, with the maximum occurring at the northern fringe of the Alps (Dittmar *et al.*, 2006). Radial growth rates had fully recovered in 2017 with no visible long-term effects of the late spring frost event in 2016, showing the high resilience to late frost of beech (Dittmar *et al.*, 2006; Principe *et al.*, 2017). However, as shown in D'Andrea *et al*. (2019), beech trees during 2016 were able to compensate for reserve lost, completely refilling the pool at the same level as before the frost event. Hence, it were not need to prioritize reserve recharge over stem biomass production the subsequent year.

Surprisingly, the 2017 summer drought shown no effect on the stem radial growth, we can only hypothesis that because it occurred when trees already completed the primary of the processes, as already demonstrated in the Mediterranean region for other tree species (Forner *et al.*, 2018).

Effluxes from stem are not entirely synchronised to radial growth

Mean annual values of Q_{10} ranged between 2.11 (2016) to 2.71 (2015) and were similar to the values estimated at the same site for co-dominant (2.59) and dominant (2.34) beech trees (Guidolotti *et al.*, 2013). Q_{10nw}, and Q_{10w} estimated in this study are very comparable with the dataset of various coniferous and broadleaf tree species reported in Damesin et al.(2002). Similar intra-annual variability of Q_{10} were observed in many studies on different species with higher Q_{10} during the growing period (Paembonan *et al.*, 1992; Carey *et al.*, 1997; Stockfors & Linder, 1998; Gruber *et al.*, 2009). However, other studies found stable Q_{10} throughout the year (Ceschia *et al.*, 2002; Damesin *et al.*, 2002).

As reported in other studies, ES15, stemCO_2 efflux at an air temperature of 15°C, was sensitive to wood formation processes, showing an increase during the growing period (Ceschia *et al.*, 2002; Damesin *et al.*, 2002).

Maximal xylem production and maximum ES were not synchronized while a constant delay of about a month was observed, as in young beech forest where the peak of ES occurred *c*. 27 days after the maximum stem growth rate (Ceschia *et al.*, 2002). Furthermore, our results confirmed that at the peak ES occurred when xylem cells were still in the phase of wall thickening and lignification, as previously hypothesized (Ceschia *et al.*, 2002). Moreover, when maximum ES was observed, it is very likely that trees were already refilling the stem C reserves pool (Scartazza *et al.*, 2013).

Only spring frost affects negatively stem C fluxes

The amount of C fixed by stem biomass formation in 2015 and 2017 ranged from 1.47 to 1.65 Mg C ha^{-1} yr^{-1}, thus being at the low end of values reported for a beech forest in Germany from 1.69 to 2.41 Mg C ha^{-1} yr^{-1} (Mund *et al.*, 2010). Such differences can be explained by differences in environmental conditions. In 2016, however, we measured only 0.194 ± 0.05 Mg C ha^{-1} yr^{-1}, i.e. only about 20% of the fixation during the two reference years, emphasizing how exceptionally negative this year was.

Annual stem CO_2 efflux (AES) is known to be highly variable in temperate forests (Yang *et al.*, 2016). Our data ranges from 0.662 to 0.938 Mg C ha^{-1} yr^{-1} and thus is lower than the 1.65 to 2.25 Mg C ha^{-1} yr^{-1} reported for a younger beech forest (Damesin *et al.*, 2002).

Annual stem CO_2 efflux (AES) is known to be highly variable in temperate forests (Yang *et al.*, 2016). Our data ranges from 0.66 to 0.94 Mg C ha^{-1} yr^{-1} and thus is lower than the 1.65 to 2.25 Mg C ha^{-1} yr^{-1} reported for a younger beech forest (Damesin *et al.*, 2002).

An earlier estimate for AES at the study site was 0.63 Mg C ha^{-1} yr^{-1} (Guidolotti *et al.*, 2013) for 2007, another year characterized by a summer drought. The stem C efflux of the drought year presented in this study (2017, 0.85 Mg C ha^{-1} yr^{-1}) was about 25% higher than 2007, this could be due to an increase of stem biomass (*c*. 15% lower in 2007 than in 2017, see also Collalti *et al*., 2019) and to different measurement tools. In 2015, the contribution of AESg to the annual stem effluxes (about 25%) was lower than that measured in a young beech forest (Ceschia et al., 2002), evidencing the importance of forest developmental stage in determining wood formation and growth respiration. The construction cost (0.23 g C fixed per g C emitted) is in the lower end of the range reported for boreal tree species (0.25 - 0.76 g C g^{-1} C (Lavigne & Ryan, 1997).

While the late frost event in 2016 reduced both wood growth and stem CO2 efflux with respect to those measured in the other two years, the percentage reduction of growth (80%) was much larger than the reduction of ES (25%). Hence, it seems that in beech the contribution of growth respiration on total stem CO_2 fluxes in mature beech trees is lower than that of maintenance respiration. In the year of late frost, the strong reduction of fixed growth C and the contemporary lower reduction of stem CO_2 efflux strongly affected the overall stem carbon balance, transforming the stems from a sink into a source of carbon. We estimated the amount of carbon released into the atmosphere by stems in 2016 equal to the amount of C fixed during the other two experimental years.

Differently, the summer drought did not have any significant effect on stem growth and neither on effluxes of C related to growth respiration. The pressure of extreme events on carbon cycle can become also evident at large scale, as shown in the case of the heat wave occurred in the summer of 2003, when the cumulative European carbon sequestration of the previous five years was released in few months (Ciais *et al.*, 2005). Forest ecosystems are potentially susceptible to all climate extremes (Reichstein *et al.*, 2013), although their impact on different functional processes may differ.

In conclusion, this study highlights the sensitivity of beech in the Mediterranean region to leaf damage as a result of post-leaf out frost. Expecting leaf development to start earlier due to global warming, is increasing the likelihood that spring frost may damage leaves. We demonstrated that stem growth was significantly reduced due to the prolonged absence of photosynthesizing leaves, despite the fact that the cambium was kept active during the leafless period by using old reserves. However, the loss in growth was not completely compensated for after re-growth of leaves, but rather the cambium activity ceased shortly thereafter. Consequently, trees fixed less C in stem biomass, with a reduction of the stem carbon efflux

484 due to growth respiration, which was mirrored also on the annual stem C effluxes. The
485 reduction of C fixation was higher than the reduction C effluxes of stem, hence, this
486 component of forest ecosystem became an active source of C, releasing in the atmosphere an
487 amount of carbon equal to the sum of the net gain of the other two study years. It can be
488 inferred that this occurred also in other beech stands similarly affected by spring frost in the
489 Centre and South of Italy.
490

491 Acknowledgements

492 The activities of Negar Rezaie at the wood anatomy laboratory of Slovenian Forestry Institute
493 were supported by the Excellence Research Award of the National Research Council of Italy,
494 Department of Biology, Agriculture, and Food Secures (Prot. 71951, 06/11/2017).
495 Collelongo-Selva Piana is one of the sites of the Italian Long Term Ecological Research
496 network (LTER-Italy), part of the International LTER network (ILTER). Research at the site
497 in the years of this study was funded by eLTER H2020 project (grant agreement no. 654359).

498 Author contribution

499 E.D'A., N.R., G.M. contributed to the design of the research. Fieldwork was carried out by
500 E.D'A., N.R.; laboratory analysis for wood formation N.R., J.M., P.P.; data analysis was done
501 by E.D'A.; data interpretation by E.D'A., N.R., P.P., J.M., A.C., G.M., J.K.. The manuscript
502 was written by E.D'A and N.R. with major contributions by P.P., J.M., A.C., G.M., J.K..
503

504 References

505 Allevato E, Saulino L, Cesarano G, Chirico GB, D'Urso G, Falanga Bolognesi S, Rita A,
506 Rossi S, Saracino A, Bonanomi G. 2019. Canopy damage by spring frost in European
507 beech along the Apennines: effect of latitude, altitude and aspect. *Remote Sensing of*
508 *Environment* 225: 431–440.
509
510 Bascietto M, Bajocco S, Mazzenga F, Matteucci G. 2018. Assessing spring frost effects on
511 beech forests in Central Apennines from remotely-sensed data. *Agricultural and Forest*
512 *Meteorology* 248: 240–250.
513
514 Bascietto M, Cherubini P, Scarascia-Mugnozza G. 2004. Tree rings from a European beech
515 forest chronosequence are useful for detecting growth trends and carbon sequestration.
516 *Canadian Journal of Forest Research* 34: 481–492.
517
518 Bascietto M, De Cinti B, Matteucci G, Cescatti A. 2012. Biometric assessment of
519 aboveground carbon pools and fluxes in three European forests by Randomized Branch
520 Sampling. *Forest Ecology and Management* 267: 172–181.
521
522 Begum S, Nakaba S, Oribe Y, Kubo T, Funada R. 2007. Induction of Cambial Reactivation

523 by Localized Heating in a Deciduous Hardwood Hybrid Poplar (Populus sieboldii 3 P .
524 grandidentata). *Annals of botany*, 439–447.
525
526 Bloemen J, Agneessens L, Van Meulebroek L, Aubrey DP, Mcguire MA, Teskey RO, Steppe
527 K. 2014. Stem girdling affects the quantity of CO_2 transported in xylem as well as CO_2
528 efflux from soil. *New Phytologist* 201: 897–907.
529 Bloemen J, McGuire MA, Aubrey DP, Teskey RO, Steppe K. 2013. Transport of root-
530 respired CO 2 via the transpiration stream affects aboveground carbon assimilation and CO
531 $_2$ efflux in trees. *New Phytologist* 197: 555–565.
532
533 Bowman WP, Barbour MM, Turnbull MH, Tissue DT, Whitehead D, Griffin KL, Bowman
534 WP. 2005. Sap flow rates and sapwood density are critical factors in within- and between-
535 tree variation in CO_2 efflux from stems of mature Dacrydium cupressinum trees. *New*
536 *Phytologist* 167: 815–828.
537
538 Campioli M, Verbeeck H, Van den Bossche J, Wu J, Ibrom A, D'Andrea E, Matteucci G,
539 Samson R, Steppe K, Granier A. 2013. Can decision rules simulate carbon allocation for
540 years with contrasting and extreme weather conditions? A case study for three temperate
541 beech forests. *Ecological Modelling* 263.
542
543 Carey E V., Callaway RM, DeLucia EH. 1997. Stem respiration of ponderosa pines grown in
544 contrasting climates: implications for global climate change. *Oecologia* 111: 19–25.
545
546 Carrer M, Brunetti M, Castagneri D. 2016. The Imprint of Extreme Climate Events in
547 Century-Long Time Series of Wood Anatomical Traits in High-Elevation Conifers.
548 *Frontiers in Plant Science* 7: 1–12.
549
550 Ceschia É, Damesin C, Lebaube S, Pontailler JY, Dufrêne É. 2002. Spatial and seasonal
551 variations in stem respiration of beech trees (*Fagus sylvatica*). *Annals of Forest Science*
552 59: 801–812.
553
554 Chan T, Berninger F, Kolari P, Nikinmaa E, Hölttä T. 2018a. Linking stem growth respiration
555 to the seasonal course of stem growth and GPP of Scots pine. *Tree Physiology* 38: 1356–
556 1370.
557
558 Chan T, Berninger F, Kolari P, Nikinmaa E, Hölttä T. 2018b. Linking stem growth respiration
559 to the seasonal course of stem growth and GPP of Scots pine. *Tree Physiology*: 1356–1370.
560
561 Chiti T, Papale D, Smith P, Dalmonech D, Matteucci G, Yeluripati J, Rodeghiero M,
562 Valentini R. 2010. Predicting changes in soil organic carbon in mediterranean and alpine
563 forests during the Kyoto Protocol commitment periods using the CENTURY model. *Soil*
564 *Use and Management* 26: 475–484.
565
566 Collalti A, Marconi S, Ibrom A, Trotta C, Anav A, *et al*. 2016. Validation of 3D-CMCC
567 Forest Ecosystem Model (v.5.1) against eddy covariance data for 10 European forest sites.
568 *Geoscientific Model Development* 9: 479–504.
569
570 Collalti A, Tjoelker MG, Hoch G, Mäkelä A, Guidolotti G, *et al*. 2019. Plant respiration:
571 Controlled by photosynthesis or biomass? *Global Change Biology*,
572 https://doi.org/10.1111/gcb.14857.

Collalti A, Trotta C, Keenan TF, Ibrom A, Bond-lamberty B, *et al*. 2018. Thinning Can Reduce Losses in Carbon Use Efficiency and Carbon Stocks in Managed Forests Under Warmer Climate. *Journal of Advances in Modeling Earth Systems* 10: 2427–2452.

Čufar K, Prislan P, De Luis M, Gričar J. 2008. Tree-ring variation, wood formation and phenology of beech (*Fagus sylvatica*) from a representative site in Slovenia, SE Central Europe. *Trees - Structure and Function* 22: 749–758.

Cuny HE, Rathgeber CBK, Frank D, Fonti P, Mäkinen H, *et al*. 2015. Woody biomass production lags stem-girth increase by over one month in coniferous forests. *Nature Plants* 1: 15160.

D'Andrea E, Rezaie N, Battistelli A, Gravichkova O, Kuhlmann I, *et al*. 2019. Winter's bite: Beech trees survive complete defoliation due to spring late frost damage by mobilizing old C reserves. *New Phytologist*, 224: 625–631

Damesin C, Ceschia E, Le Goff N, Ottorini J-M, Dufrêne E. 2002. Stem and branch respiration of beech: from tree measurements to estimations at the stand level. *New Phytologist* 153: 159–172.

Deslauriers A, Rossi S, Anfodillo T, Saracino A. 2008. Cambial phenology, wood formation and temperature thresholds in two contrasting years at high altitude in southern Italy. *Tree physiology* 28: 863–871.

Dittmar C, Fricke W, Elling W. 2006. Impact of late frost events on radial growth of common beech (*Fagus sylvatica* L.) in Southern Germany. *European Journal of Forest Research* 125: 249–259.

Forner A, Valladares F, Bonal D, Granier A, Grossiord C. 2018. Extreme droughts affecting Mediterranean tree species' growth and water-use efficiency: the importance of timing. *Tree physiology*.

Frank D, Reichstein M, Bahn M, Thonicke K, Frank D, Mahecha MD, Smith P, van der Velde M, Vicca S, Babst F, *et al.* 2015. Effects of climate extremes on the terrestrial carbon cycle: Concepts, processes and potential future impacts. *Global Change Biology* 21: 2861–2880.

Gazol A, Camarero JJ, Colangelo M, de Luis M, Martínez del Castillo E, Serra-Maluquer X. 2019. Summer drought and spring frost, but not their interaction, constrain European beech and Silver fir growth in their southern distribution limits. *Agricultural and Forest Meteorology* 278: 107695.

Gordo O, Sanz JJ. 2010. Impact of climate change on plant phenology in Mediterranean ecosystems. *Global Change Biology* 16: 1082–1106.

Greco S, Infusino M, De Donato C, Coluzzi R, Imbrenda V, Lanfredi M, Simoniello T, Scalercio S. 2018. Late spring frost in mediterranean beech forests: Extended crown dieback and short-term effects on moth communities. *Forests* 9: 1–18.

623 Gričar J, Krže L, Čufar K. 2009. Number of cells in xylem, phloem and dormant cambium in
624 silver fir (ABIES ALBA), in trees of different vitality. *IAWA Journal*, 30: 121–133.
625
626 Gruber A, Wieser G, Oberhuber W. 2009. Intra-annual dynamics of stem CO_2 efflux in
627 relation to cambial activity and xylem development in Pinus cembra. *Tree Physiology* 29:
628 641–649.
629 Guidolotti G, Rey A, D'Andrea E, Matteucci G, De Angelis P. 2013. Effect of environmental
630 variables and stand structure on ecosystem respiration components in a Mediterranean
631 beech forest. *Tree Physiology* 33: 960–972.
632
633 Hilman B, Muhr J, Trumbore SE, Kunert N, Carbone MS, *et al.* 2019. Comparison of CO_2
634 and O_2 fluxes demonstrate retention of respired CO_2 in tree stems from a range of tree
635 species. *Biogeosciences* 16: 177–191.
636
637 Lavigne MB, Ryan MG. 1997. Growth and maintenance respiration rates of aspen , black
638 spruce and jack pine stems at northern and southern BOREAS sites. *Tree Physiology*: 543–
639 552.
640
641 Linares JC, Camarero JJ, Carreira JA. 2009. Plastic responses of Abies pinsapo xylogenesis to
642 drought and competition. *Tree Physiology* 29: 1525–1536.
643
644 Merganičová K, Merganič J, Lehtonen A, Vacchiano G, *et al*. 2019. Forest carbon allocation
645 modelling under climate change. *Tree Physiology* doi: 10.1093/treephys/tpz105
646
647 Michelot A, Simard S, Rathgeber C, Dufrêne E, Damesin C. 2012. Comparing the intra-
648 annual wood formation of three European species (*Fagus sylvatica*, *Quercus petraea* and
649 *Pinus sylvestris*) as related to leaf phenology and non-structural carbohydrate dynamics.
650 *Tree Physiology* 32: 1033–1045.
651
652 Mund M, Kutsch WL, Wirth C, Kahl T, Knohl A, Skomarkova M V, Schulze E-D. 2010. The
653 influence of climate and fructification on the inter-annual variability of stem growth and
654 net primary productivity in an old-growth, mixed beech forest. *Tree physiology* 30: 689–
655 704.
656
657 Nolè A, Rita A, Ferrara AMS, Borghetti M. 2018. Effects of a large-scale late spring frost on
658 a beech (*Fagus sylvatica* L.) dominated Mediterranean mountain forest derived from the
659 spatio-temporal variations of NDVI. *Annals of Forest Science* 75: 83.
660
661 Oladi R, Pourtahmasi K, Eckstein D, Bräuning A. 2011. Seasonal dynamics of wood
662 formation in Oriental beech (*Fagus orientalis* Lipsky) along an altitudinal gradient in the
663 Hyrcanian forest, Iran. *Trees - Structure and Function* 25: 425–433.
664
665 Paembonan SA, Hagihara A, Hozumi K. 1992. Long-Term respiration in relation to growth
666 and maintenance processes of the aboveground parts of a hinoki forest tree. *Tree*
667 *Physiology* 10: 21–31.
668
669 Peuke AD, Schraml C, Hartung W, Rennenberg H. 2002. Identification of drought-sensitive
670 beech ecotypes by physiological parameters. *New Phytologist* 154: 373–387.
671
672 Principe A, Struwe T, Wilmking M, Kreyling J. 2017. Low resistance but high resilience in

673 growth of a major deciduous forest tree (*Fagus sylvatica* L.) in response to late spring frost
674 in southern Germany. *Trees - Structure and Function* 31: 743–751.
675
676 Prislan P, Čufar K, De Luis M, Gričar J. 2018. Precipitation is not limiting for xylem
677 formation dynamics and vessel development in European beech from two temperate forest
678 sites. *Tree Physiology* 38: 186–197.
679 Prislan P, Gričar J, De Luis M, Smith KT, Cufar K. 2013. Phenological variation in xylem
680 and phloem formation in *Fagus sylvatica* from two contrasting sites. *Agricultural and*
681 *Forest Meteorology*: 142–151.
682
683 R Development Core Team. 2018. R: A Language and Environment for Statistical
684 Computing.
685
686 Rathgeber CBK, Rossi S, Bontemps J-D. 2011. Cambial activity related to tree size in a
687 mature silver-fir plantation. *Annals of Botany* 108: 429–438.
688
689 Rathgeber CBK, Santenoise P, Cuny HE. 2018. CAVIAR: An R package for checking,
690 displaying and processing wood-formation-monitoring data. *Tree Physiology* 38: 1246–
691 1260.
692
693 Rezaie N, D'Andrea E, Bräuning A, Matteucci G, Bombi P, Lauteri M. 2018. Do atmospheric
694 CO_2 concentration increase, climate and forest management affect iWUE of common
695 beech? Evidences from carbon isotope analyses in tree rings. *Tree Physiology* 1975: 1110–
696 1126.
697
698 Saveyn A, Steppe K, Mc Guire MA, Lemeur R, Teskey RO. 2008. Stem respiration and
699 carbon dioxide efflux of young Populus deltoides trees in relation to temperature and
700 xylem carbon dioxide concentration. *Oecologia* 154: 637–649.
701
702 Scarascia-Mugnozza G, Bauer GA, Persson H, Matteucci G, Masci A. 2000. Tree Biomass,
703 Growth and Nutrient Pools. In: Schulze E-D, *ed*. Carbon and Nitrogen Cycling in
704 European Forest Ecosystems. Springer Verlag, 49–62.
705
706 Scartazza A, Moscatello S, Matteucci G, Battistelli A, Brugnoli E. 2013. Seasonal and inter-
707 annual dynamics of growth, non-structural carbohydrates and C stable isotopes in a
708 Mediterranean beech forest. *Tree physiology* 33: 730–42.
709
710 Schröter D, Cramer W, Leemans R, Prentice IC, Araújo MB, Arnell NW, Bondeau A,
711 Bugmann H, Carter TR, Gracia CA, *et al.* 2005. Ecosystem service supply and
712 vulnerability to global change in Europe. *Science (New York, N.Y.)* 310: 1333–7.
713
714 Schume H, Grabner M, Eckmüllner O. 2004. The influence of an altered groundwater regime
715 on vessel properties of hybrid poplar. *Trees* 18: 184–194.
716
717 Stockfors J, Linder S. 1998. Effect of nitrogen on the seasonal course of growth and
718 maintenance respiration in stems of Norway spruce trees. *Tree Physiology* 18: 155–166.
719
720 Teskey RO, Saveyn A, Steppe K, McGuire MA. 2008. Origin, fate and significance of CO_2 in
721 tree stems. *New Phytologist* 177: 17–32.
722

723 Trumbore SE, Angert A, Kunert N, Muhr J, Chambers JQ. 2013. What's the flux? Unraveling
724 how CO_2 fluxes from trees reflect underlying physiological processes. *New Phytologist*
725 197: 353–355.
726
727 Ubierna N, Kumar AS, Cernusak LA, Pangle RE, Gag PJ, Marshall JD. 2009. Storage and
728 transpiration have negligible effects on δ13C of stem CO_2 efflux in large conifer trees.
729 *Tree Physiology* 29: 1563–1574.
730
731 Vitasse Y, Schneider L, Rixen C, Christen D, Rebetez M. 2018. Increase in the risk of
732 exposure of forest and fruit trees to spring frosts at higher elevations in Switzerland over
733 the last four decades. *Agricultural and Forest Meteorology* 248: 60–69.
734
735 Yang J, He Y, Aubrey DP, Zhuang Q, Teskey RO. 2016. Global patterns and predictors of
736 stem CO_2 efflux in forest ecosystems. *Global Change Biology* 22: 1433–1444.
737
738 Zhang X, Friedl M a., Schaaf CB, Strahler AH, Hodges JCF, Gao F, Reed BC, Huete A.
739 2003. Monitoring vegetation phenology using MODIS. *Remote Sensing of Environment*
740 84: 471–475.
741
742
743
744
745
746
747
748

Figure

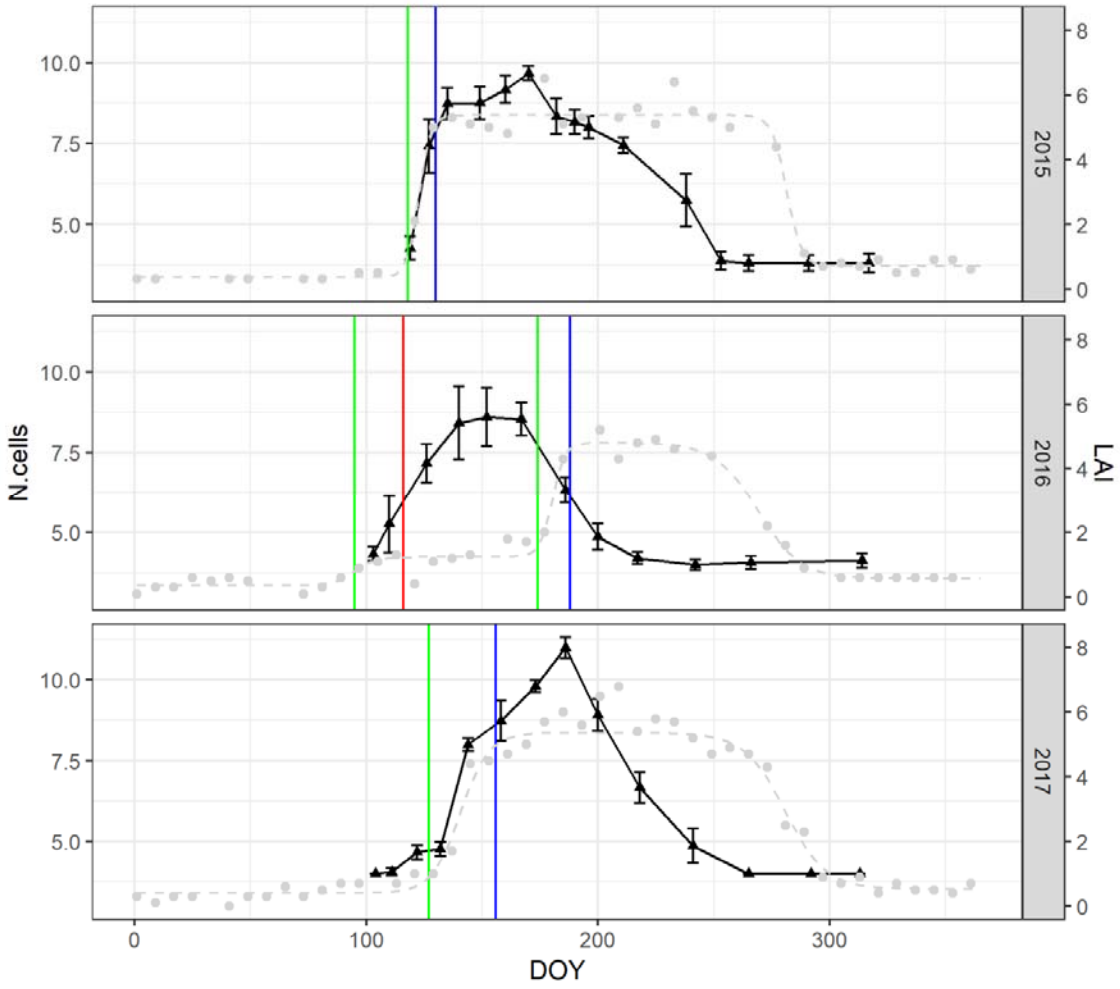

Fig. 1: Number of cambium cells (N. cells vs. Leaf area index (LAI, m^2m^{-2}). Grey points and dashed lines are the MODIS-LAI values and modelled intra-annual dynamic of Selva Piana beech forest, respectively. Green and blue vertical lines represent the green up and maturity phase of leaf phenology, respectively. Red vertical line represents the late frost of 25th April 2016. Black triangles are the average number of cambial cells of five beech trees. Bars are the standard error.

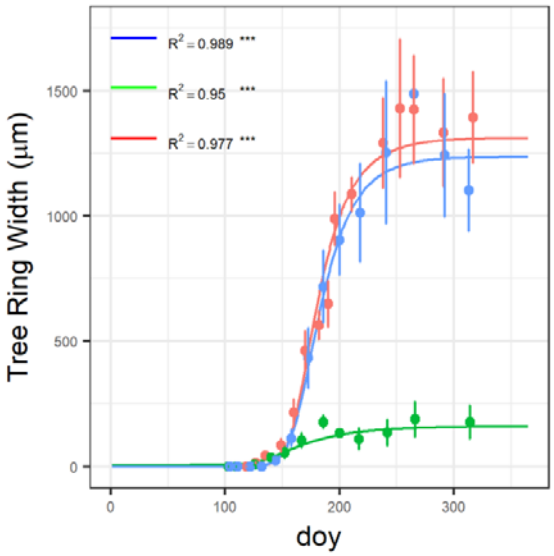

Fig. 2: Intra-annual dynamics of xylem formation (µm) in 2015 (red dots and solid line), 2016 (green dots and solid line) and 2017 (blue dots and solid line). Gompertz functions were fitted to the total xylem increment comprised of enlarging, wall thickening and mature cells. Each point is the mean of the 5 sampled *Fagus sylvatica* trees and bars are standard errors. * *p*-value < 0.001**

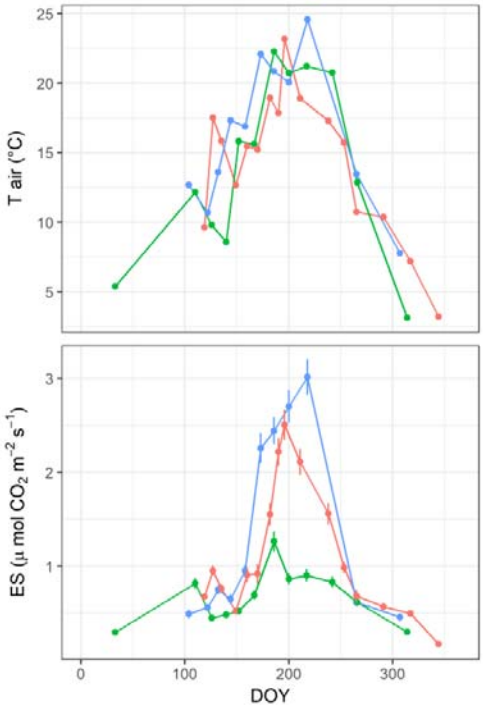

Fig. 3: Top panel: T_{air} (°C) at the measuring time in 2015 (Red), 2016 (Green), and 2017 (Blue). Bottom panel: Measured stem CO_2 effluxes (µmol CO_2 m^{-2} s^{-1}) in 2015 (Red), 2016 (Green), and 2017 (Blue). Each point is the mean of 5 *Fagus sylvatica* trees. Bars are standard errors.

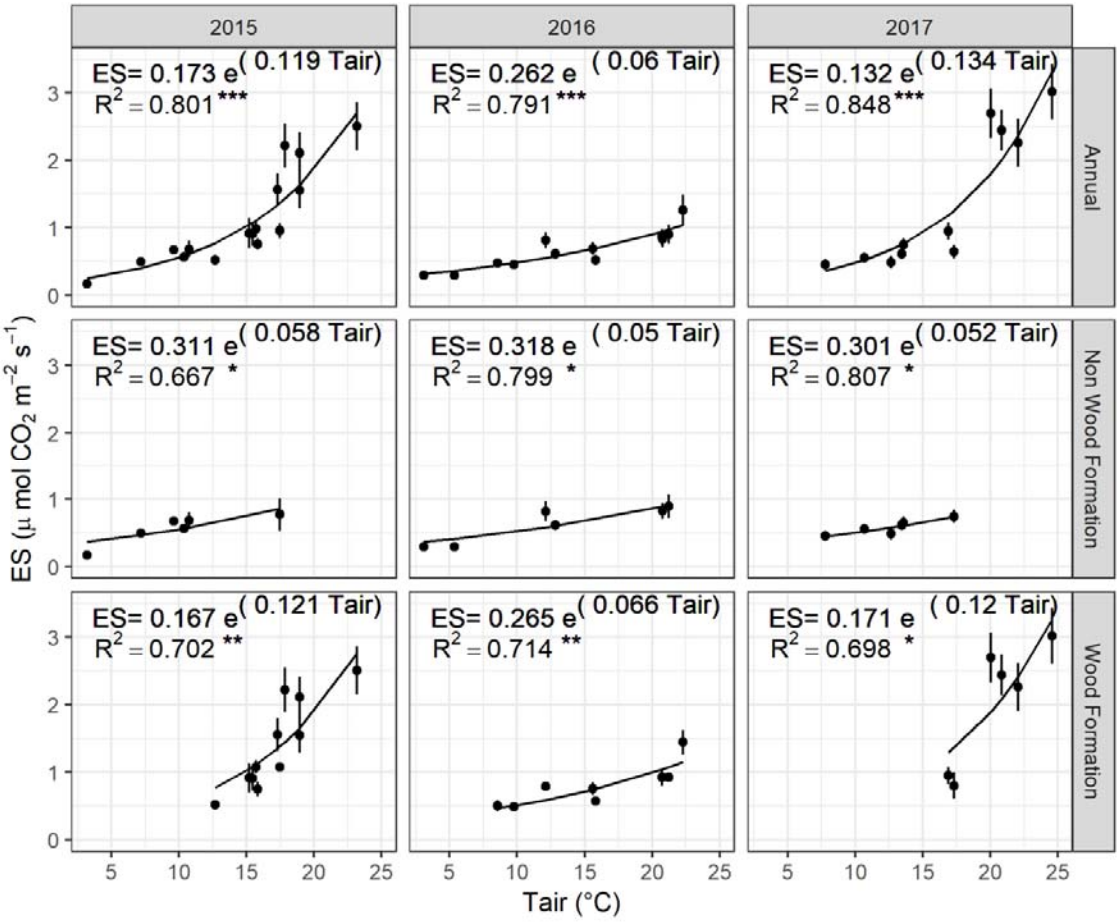

769

770 **Fig. 4: Relationship between ES (µmol CO_2 m^{-2} s^{-1}) and air temperature (T_{air}, °C). Annual,**
771 **considering the whole measurements for each year, each point is the mean of the five sampled**
772 **trees. Each point represents the mean of those trees, during non-wood and wood formation**
773 **periods, at a given sampling date. Bars are the standard error. *** *p*-value < 0.001, ** *p*-value <**
774 **0.01, * *p*-value < 0.05.**

775

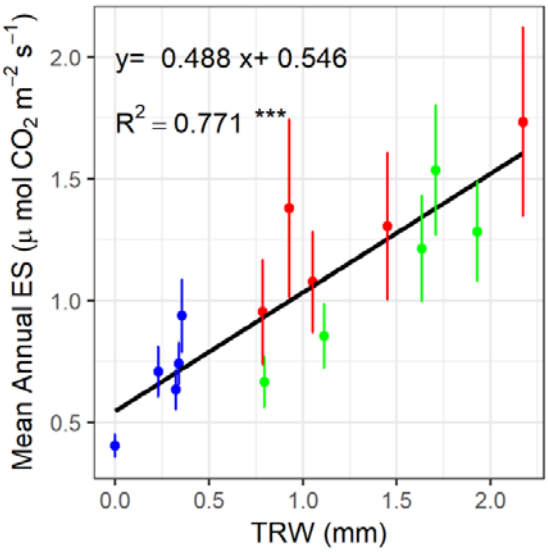

Fig. 5: Relationships between the ring widths (mm) and the mean annual ES (µmol CO_2 m^{-2} s^{-1}) measured in 2015 (Green), 2016 (Blue), and 2017 (Red). Each point represents a sampled *Fagus sylvatica* tree per year. Bars are the standard error. * *p*-value < 0.001.**

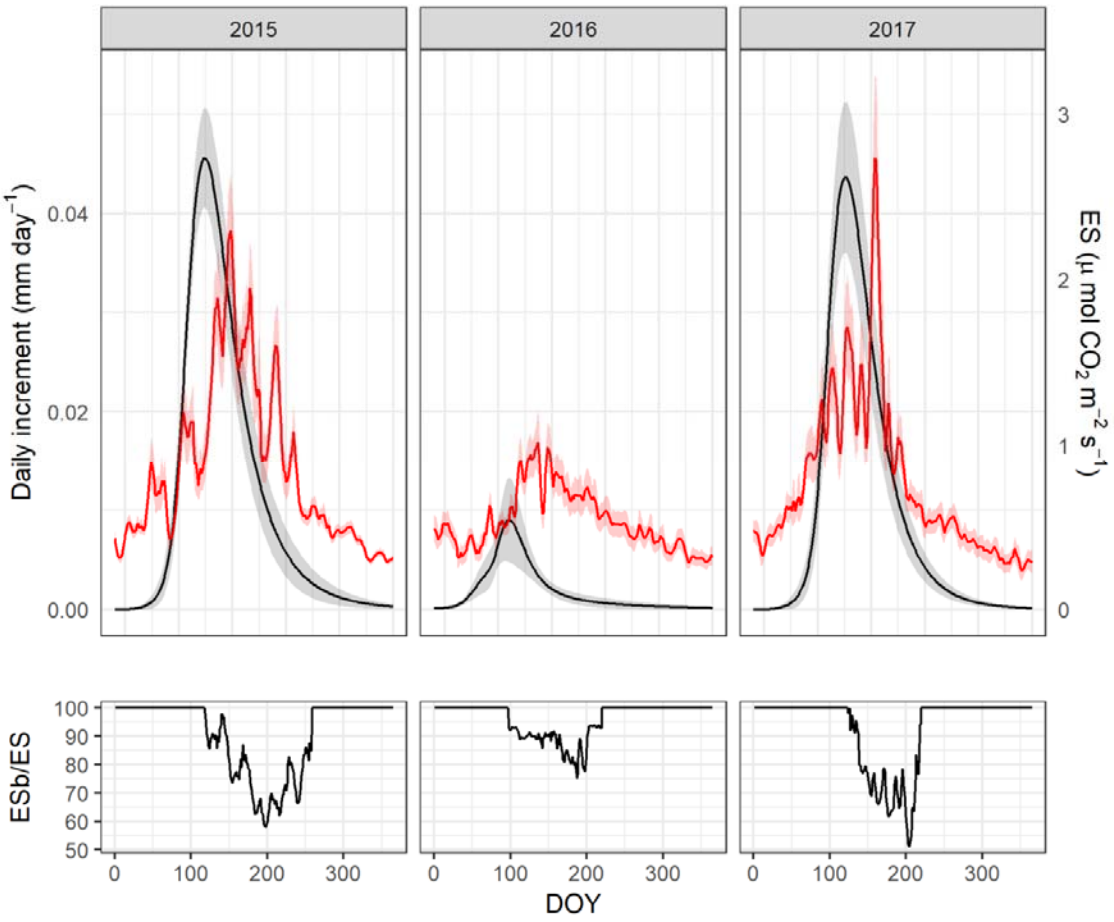

Fig. 6: Daily increment and stem Carbon effluxes of *Fagus sylvatica*. Black line is the daily increment during 2015, 2016 and 2017, respectively. Red line represents ES, the daily C effluxes. The below panel, ESb/ES shows the contribution of maintenance respiration to daily stem C efflux.

Tables

Table 1: List of terms used in the text

Terms	Definition	Spatial Scale
ES	stem CO_2 efflux per surface area ($\mu mol\ m^{-2}\ s^{-1}$)	Local
ES_{15w}	specific CO_2 efflux at an air temperature of 15°C during the wood formation period ($\mu mol\ m^{-2}\ s^{-1}$)	Local
ES_{15nw}	specific CO_2 efflux at an air temperature of 15°C during the non-wood formation period ($\mu mol\ m^{-2}\ s^{-1}$)	Local
Q_{10w}	ES temperature sensitivity for a 10 °C increase during the wood formation period	Local
Q_{10nw}	ES temperature sensitivity for a 10 °C increase during the non-wood formation period	Local
ESw	stem CO_2 efflux per surface area ($\mu mol\ m^{-2}\ s^{-1}$) during wood formation	Local
ESb	stem CO_2 efflux per surface area ($\mu mol\ m^{-2}\ s^{-1}$) due to maintenance respiration	Local
ESg	stem CO_2 efflux per surface area ($\mu mol\ m^{-2}\ s^{-1}$) due to growth respiration	Local
AES	annual stem C efflux ($Mg\ C\ ha^{-1}\ yr^{-1}$)	Stand
AESb	annual stem C efflux due to maintenance respiration ($Mg\ C\ ha^{-1}\ yr^{-1}$)	Stand
AESg	annual stem C efflux due to growth respiration ($Mg\ C\ ha^{-1}\ yr^{-1}$)	Stand
SG	annual C fixed in stem biomass ($Mg\ C\ ha^{-1}\ yr^{-1}$)	Stand

794 **Table 2: Parameters describing the intra annual radial growth derived from Gompertz function**
795 **for the total xylem increment comprised of enlarging, wall thickening and mature cells. α is the**
796 **upper asymptote, representing the final ring width at the end of the growing season; tx is the**
797 **DOY at which the daily increment is maximal (Gompertz curve inflection point); rx is the**
798 **maximal daily increment (μm day^{-1}). Different letters represent significant differences among**
799 **the monitored years.**
800

		Total xylem increment		
Parameter	Year	Mean (± S.E.)	F	*p*-value
α	2015	1312.17 (± 196.15) a		
α	2016	230.12 (± 31.54) b	13.722	< 0.01
α	2017	1234.80 (± 269.32) a		
rx	2015	25.77 (± 2.95) a		
rx	2016	6.09 (± 2.00) b	8.469	0.014
rx	2017	22.71 (± 3.51) a		
tx	2015	174 (± 2.19) a		
tx	2016	157 (± 5.65) b	22.667	< 0.001
tx	2017	174.80 (± 1.24) a		

801
802
803
804
805
806
807
808

Table 3: Annual C stem fluxes. AES is the annual stem C efflux assessed using specific parameters for wood formation (Q_{10w} and ES_{15w}) and non-wood formation periods (Q_{10nw} and ES_{15nw}); AESb is the annual stem C efflux due to maintenance respiration; AESg is the annual stem C efflux due to growth respiration; SG is the annual amount of C fixed in the stem biomass; different letters represent significant differences *p*-value < 0.05

Year	Flux type	Mean (± S.E.) Mg C ha^{-1} yr^{-1}	F	*p*-value
2015	AES	0.938(± 0.084) a		
2016	AES	0.662 (± 0.008) b	13.933	0.002
2017	AES	0.854 (± 0.104) a		
2015	AESb	0.760 (± 0.053) a		
2016	AESb	0.615 (± 0.072) b	6.270	0.023
2017	AESb	0.715 (± 0.090) a/b		
2015	AESg	0.178 (± 0.033) a		
2016	AESg	0.049 (± 0.017) b	8.310	0.009
2017	AESg	0.139 (± 0.027) a		
2015	SG	1.151 (± 0.151) a		
2016	SG	0.194 (± 0.050) b	18.620	< 0.001
2017	SG	1.031 (± 0.183) a		
2015	SG-AES	0.213 (± 0.087) a		
2016	SG-AES	−0.468 (± 0.055) b	16.838	0.001
2017	SG-AES	0.177 (± 0.105) a		